Electronic Supplementary Material (ESI) for Energy & Environmental Science.
This journal is © The Royal Society of Chemistry 2021

# Giant performance improvement of triboelectric nanogenerator system achieved by matched-inductor design

Zhao Wang[1], Qian Tang[1], Chuncai Shan[1], Yan Du[1], Wencong He[1], Shaoke Fu[1], Gui Li[1], Anping Liu[1], Wenlin Liu[2]* and Chenguo Hu[1]*

[1]Department of Applied Physics, Chongqing Key Laboratory of Soft Condensed Matter Physics and Smart Materials, State Key Laboratory of Power Transmission Equipment & System Security and New Technology, Chongqing University, Chongqing 400044, P. R. China

[2] College of Chemistry and Molecular Engineering, Peking University, Beijing, 100871, P. R. China

*Correspondence: liuwl-cnc@pku.edu.cn (W.L.), hucg@cqu.edu.cn (C.H.),

Key Words: triboelectric nanogenerator, matched inductor, energy management, energy efficiency, constant power

**Table S1**

**Summery of the used $C_{in}$ and output energy at different turn-on voltages of spark switch**

| Voltage kV) | 1 | 2 | 3 | 4 | 5 | 6 |
|---|---|---|---|---|---|---|
| $C_{in}$ (pF) | 400 | 100 | 100 | 60 | 50 | 33 |
| Energy (mJ) | 0.22 | 0.45 | 0.59 | 0.8 | 0.9 | 1.08 |

**Table S2**

**Parameters of inductors**

| Magnetic core type | $L_e$ (mm) | $A_e$ ($mm^2$) | $V_e$ (mm3) |
|---|---|---|---|
| EE16 | 38.2 | 18.6 | 672 |
| EE19 | 40.7 | 22.2 | 903 |
| EE22 | 44.1 | 36.9 | 1629 |
| EE28 | 51.7 | 82.9 | 4290 |
| EE40 | 78.4 | 144.5 | 11350 |
| R10-40 | 40.0 | 78.5 | 3141 |

**Table S3**

**Comparison on the performance after energy management with other works.**

| | References | TENG Size | Inductance | Average power | Work Frequency | Voltage |
|---|---|---|---|---|---|---|
| | | ($cm^2$) | (mH) | ($\mu W \cdot Hz^{-1}$) | (Hz) | (V) |
| 1 | Nano Energy 37, 168–176 (2017)[1] | 32.5 | 5 | 9 | ----- | ----- |
| 2 | Adv. Funct. Mater. 28, 1805216 (2018)[2] | 64 | ----- | 6.66 | ----- | ----- |
| 3 | Adv. Funct. Mater. 29, 1807241, (2019)[3] | 441 | 5 | ----- | 1 | 5 |
| 4 | Nano Energy 71, 104642 (2020)[4] | 30 | 3.3 | 76.4 | ----- | ----- |
| 5 | Energy Environ. Sci., 13, 277—285 (2020)[5] | 480 | 5 | ----- | 1 | 2.1 |
| 6 | Nat Commun. 11, 3221 (2020)[6] | 36 | 100 | 11.3 | ----- | ----- |
| 7 | Nano Energy 82, 105725 (2021)[7] | 36 | 10 | 13 | ----- | ----- |
| 8 | Nat Commun. 12, 4689 (2021)[8] | 276 | 20 | ----- | 10 | 11.2 |
| 9 | This work | 100 | 0.69 | 890 | 1 | 17 V |

In the table, **Voltage** refers to the voltage value on 100 μF capacitor charged by TENG with EM working at the marked frequency for 20 seconds.

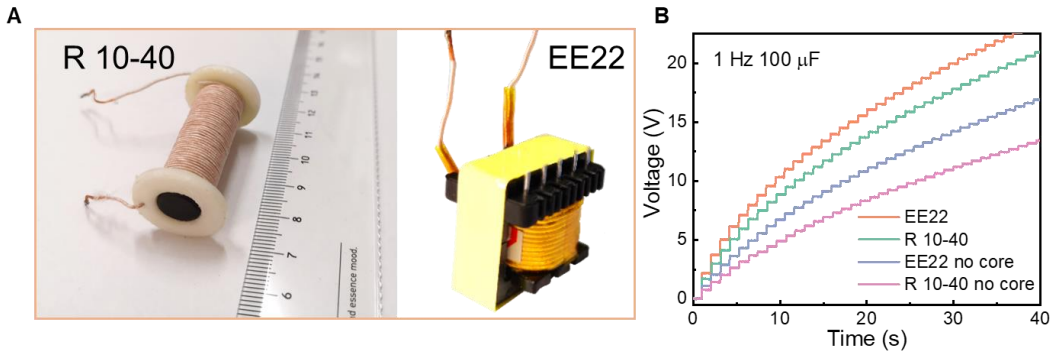


**Figure S1.** Image of inductors and output performance
(A) Image of inductor in rod type with 10 mm in diameter, 40 mm in length, R 10-40, (B) Voltage on 100 μF charged by TENG with EM in R 10-40 or EE22 inductor.

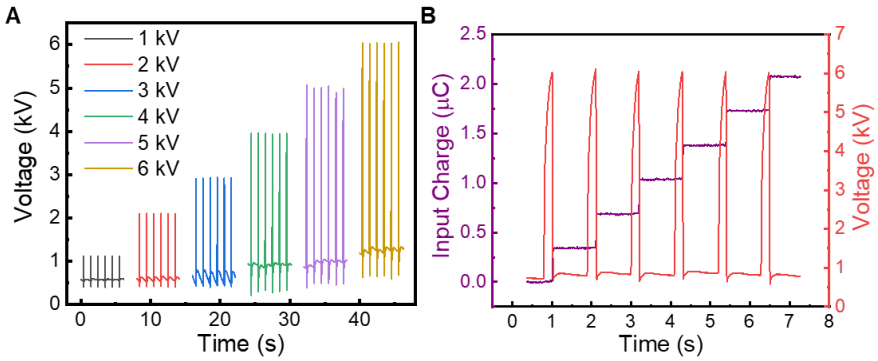


**Figure S2.** Turn-on voltage of spark switch
(A) Wave form of voltages in different value. (B) The simultaneous voltage and output charge via a spark switch.

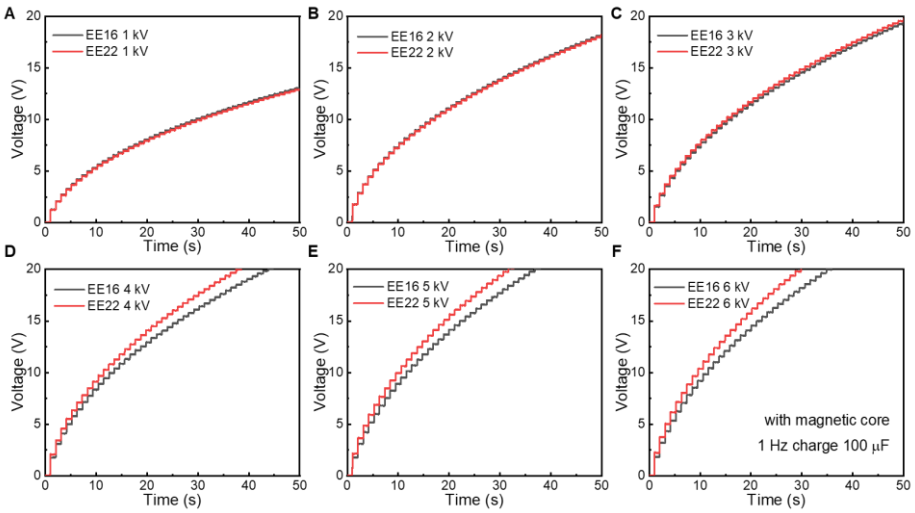


**Figure S3.** Charging performance of EE16 and EE22 at different turn-on voltages

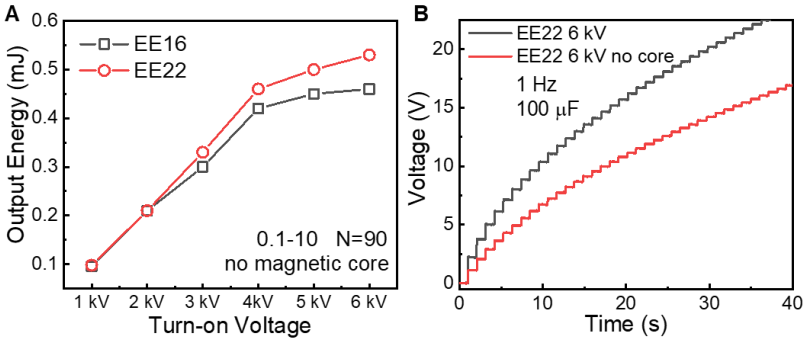


**Figure S4.** Output performance for EE16 and EE22.
(A) Comparison in output energy of TENG using EM in EE16 and EE22 inductor without magnetic core at different turn-on voltages. (B) Voltage on 100 μF charged by TENG with EM in EE22 inductor with magnetic core or not.

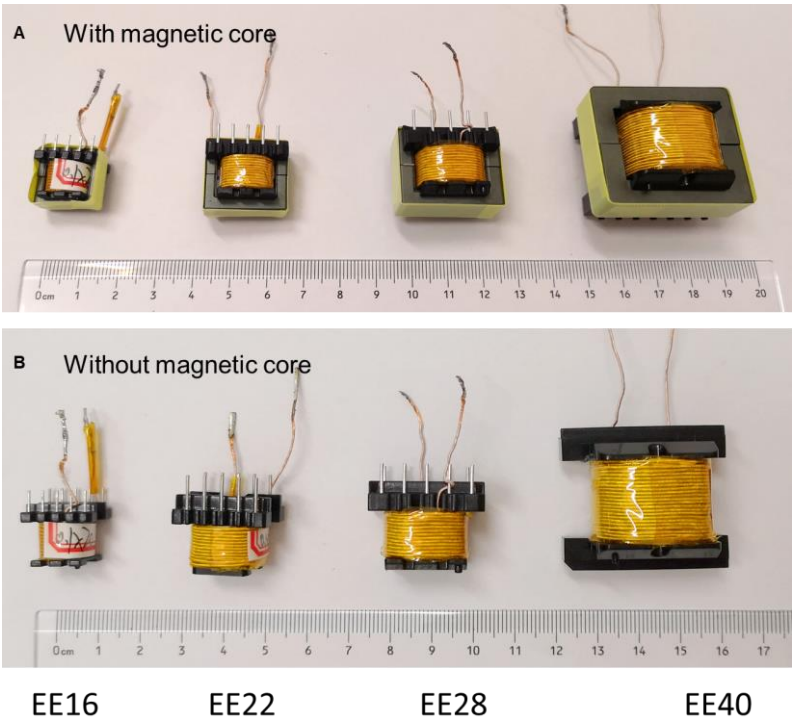


**Figure S5.** Image of inductors of EE type in different sizes. (A) EE inductors with magnetic core. (B) EE inductors without magnetic core.

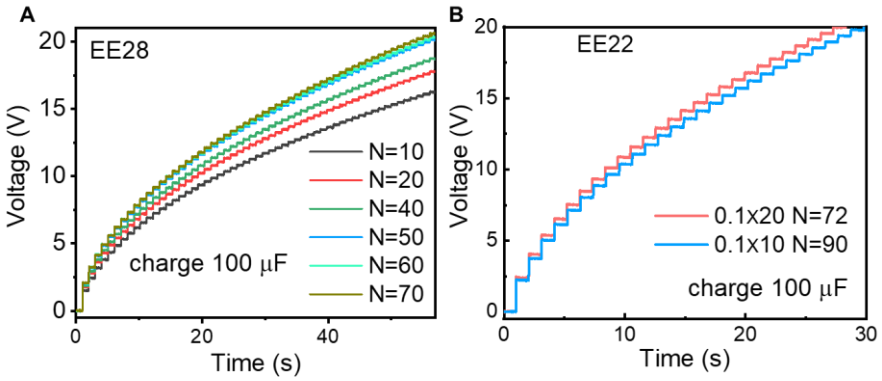


**Figure S6.** Charged voltage on 100 μF capacitor by inductors in different coil numbers. (A) Charging 100 μF capacitor using EE28 inductor with different coil numbers. (B) Charging 100 μF capacitor using EE22 inductor with 72 number of 0.1×20 wire or 90 number of 0.1×10 wire diameter.

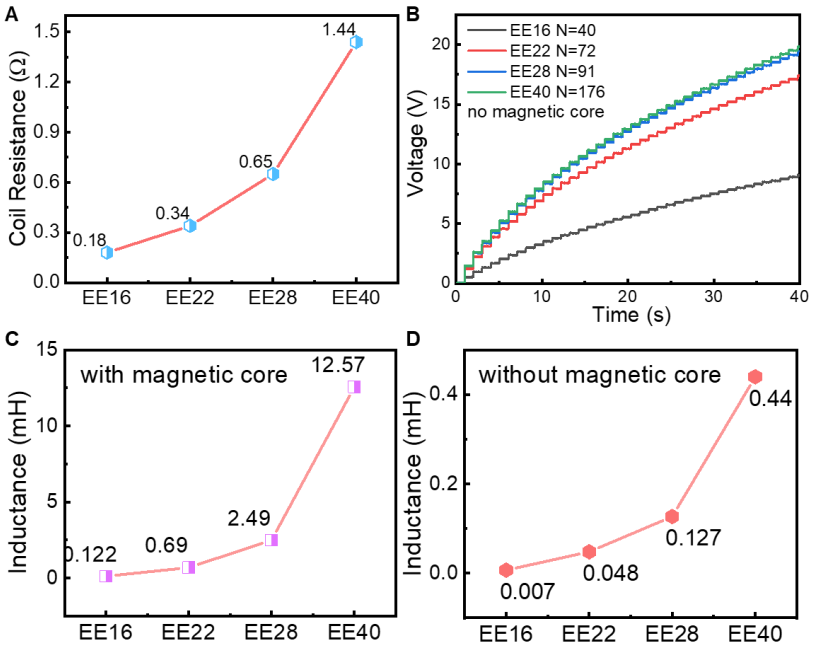


**Figure S7.** Resistance, output performance and inductance of inductors in different coil numbers. (A) The coil resistance and inductance for different sizes EE type inductor with full winding number. (B) Voltage of 100 μF charged by TENG after EM in EE type inductor and no magnetic core. (C and D) Inductance for EE type inductors with magnetic core (C) and without magnetic core (D).

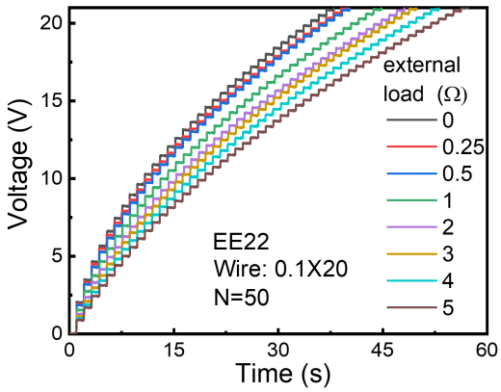


**Figure S8.** Voltage on 100 μF capacitor connecting with external loads in series.

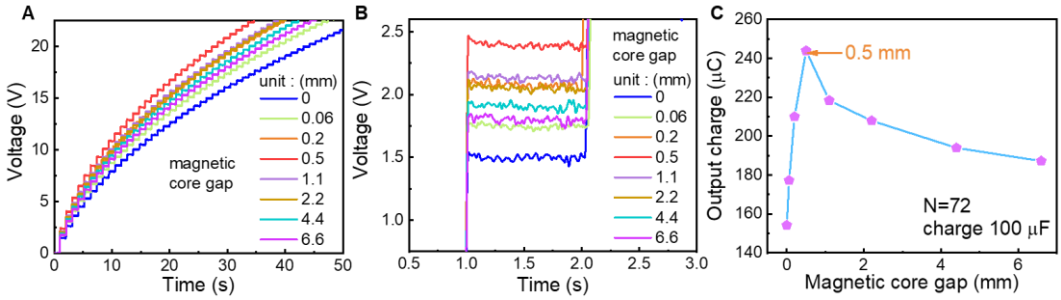


**Figure S9**. Voltage and output calculated charge under different magnetic core gaps. (A) Voltage on 100 μF capacitor charged by TENG with EM under different magnetic core gaps. (B and C) The voltage in the first cycle and the calculated output charge.

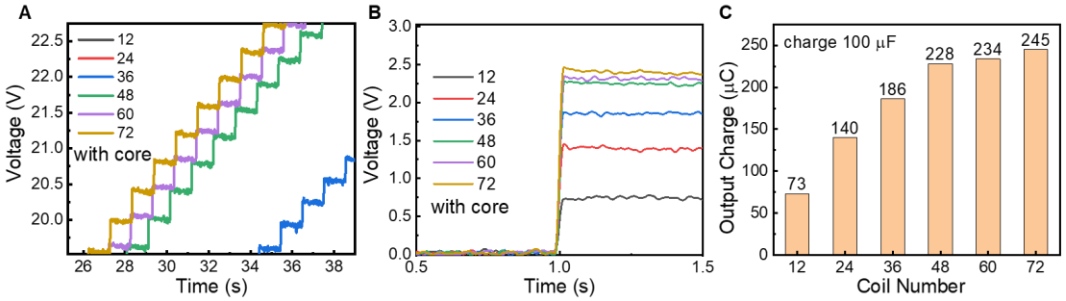


**Figure S10**. Enlarged voltage curve and output charge under different coil numbers. (A and B) The enlarged charging plot using EE22 with a magnetic core and different coil numbers in the cycles after 25 (A) and the first cycle (B). (C) The calculated output charge at different coil numbers from (B).

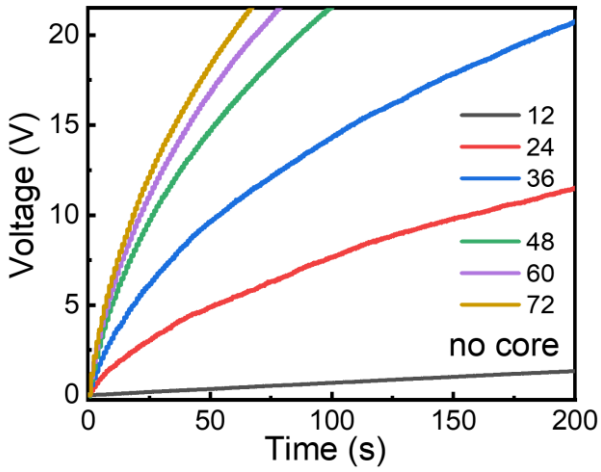


**Figure S11**. Charging 100 μF performance of TENG converted by EE22 inductor with different coil numbers and no magnetic core.

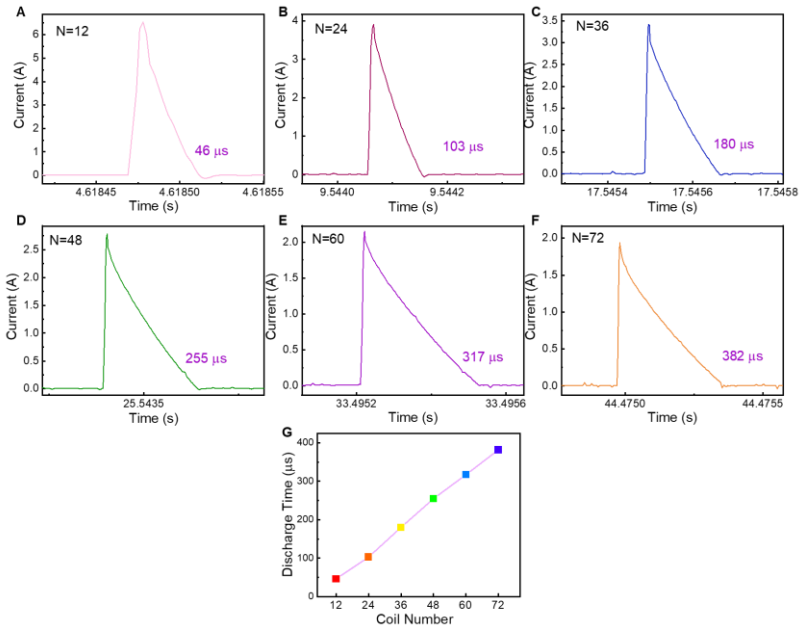


**Figure S12**. Output current and the discharging time transferring by EE22 under different winding numbers.

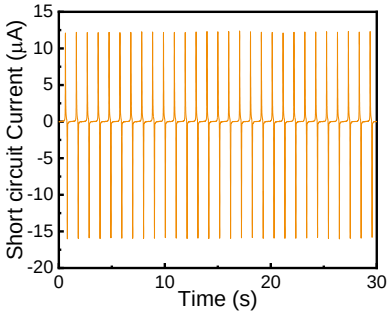


**Figure S13**. Short circuit output current from TENG directly and without EM.

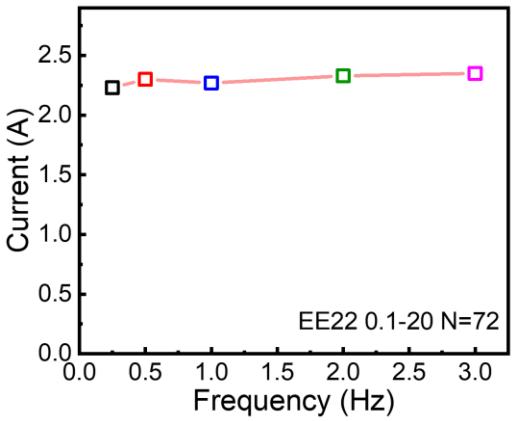


**Figure S14**. Pulse output current of TENG at different operating frequencies after being converted by EM.

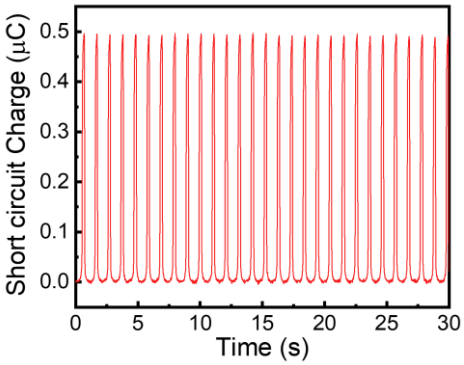


**Figure S15**. Short circuit output charge from TENG directly.

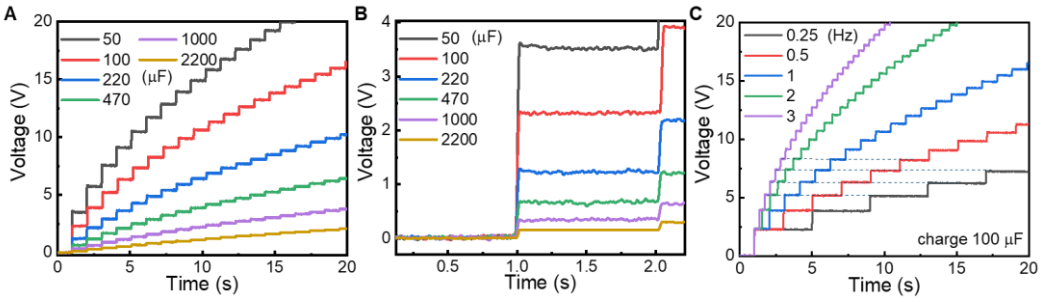


**Figure S16**. Charging capacitors in different capacitances. (A and B) The plot of charging capacitors in different capacitances the enlarged plot of the first cycle. (C) After using EM, voltage on 100 μF charged at different frequencies.

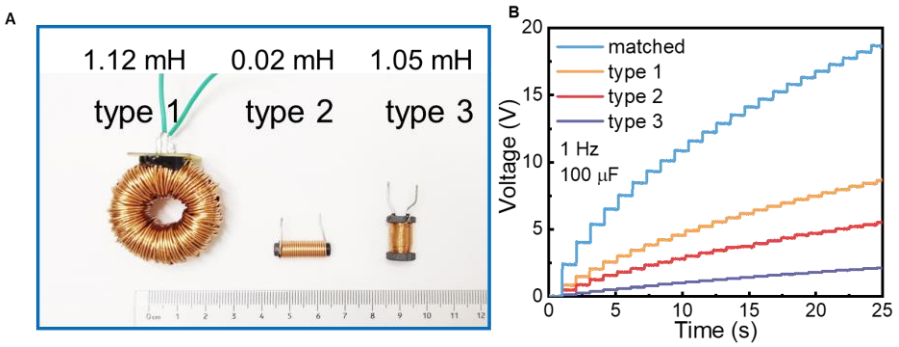


**Figure S17**. Image and performance of mismatched inductor-based EM. (A) Image of three commercial inductors with their inductance shown. (B) Comparison of charging performance of the three inductors and our matched inductor.

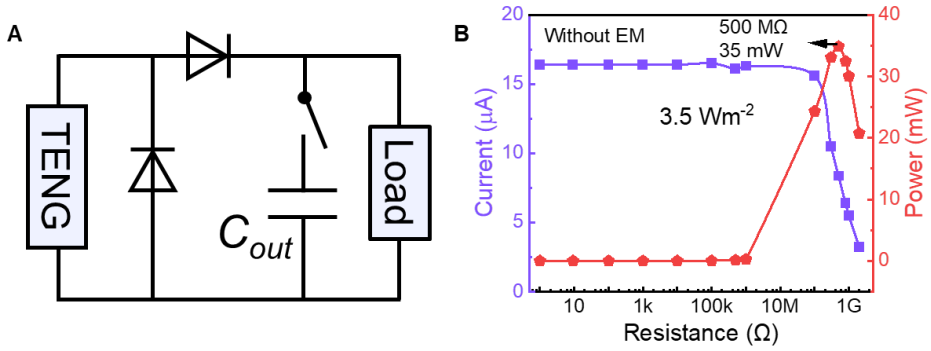


**Figure S18**. (A) Circuit schematic for measure the output pulse power and constant power from TENG without management. (B) The current and pulse power on loads driven by TENG directly.

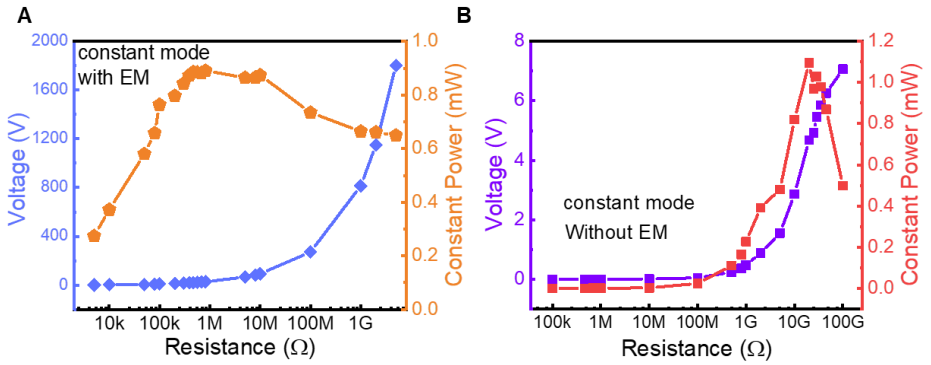


**Figure S19**. Comparison of voltage on loads at constant mode with EM and without EM. (A and B) Constant output power and voltage on different external loads powered by TENG with EM(A), or powered by TENG directly (B).

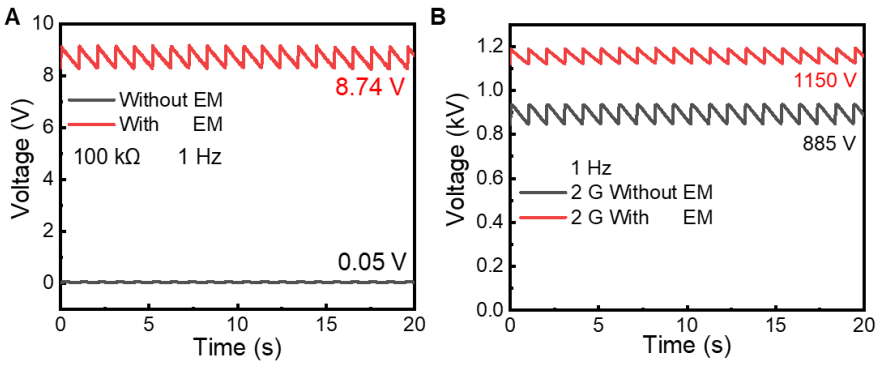


**Figure S20**. Voltage curve on loads at constant mode. (A and B) Comparison of voltage on 100 KΩ and 2 GΩ driven by TENG with EM and without EM.

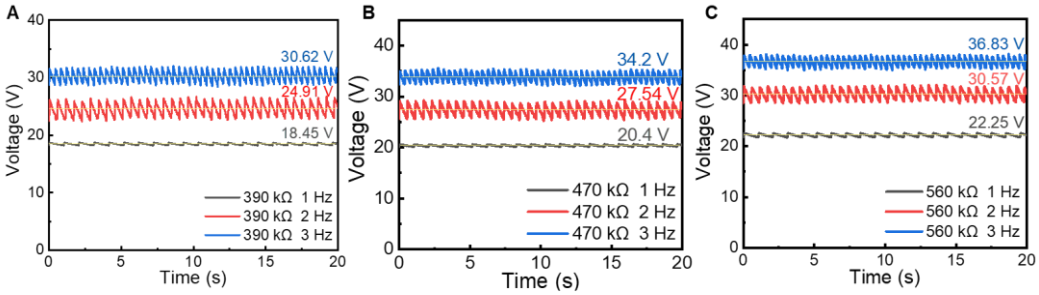


**Figure S21**. Detailed average voltage curve on loads at different operating frequencies. (A-C) Voltage cure on 390 KΩ, 470 KΩ and 560 KΩ driven by TENG with EM at different working frequencies.

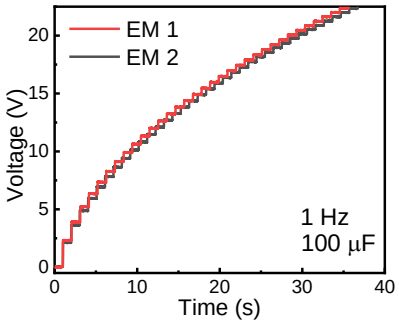


**Figure S22**. Performance comparison on charging 100 μF capacitor by TENG using EM 1 and EM 2 circuit.

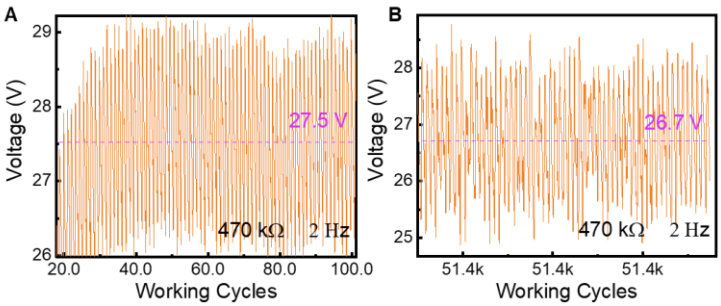


**Figure 23**. In the stability test, (A) the output voltage in the first tens cycle and (B) more than 50, 000 cycles.

**Note S1**

**Basic parameters and Discussion about duty ratio**

Here, we introduce a general inductor design strategy for the energy management (EM) using in triboelectric nanogenerator (TENG). Firstly, we introduce some common parameters in the EM unit. Then, we discuss some key design aspects like duty ratio, the size of magnetic core, diameter of copper wire, magnetic core gap, inductance and coil number of the inductor in order.

Some common parameters in the EM unit are listed as follows,

$V_{open}$, open circuit voltage of TENG

$V_B$, the turn on voltage of spark switch

$Q_{on}$, the charge flows through spark switch when it turns on

$V_{Dair}$, the air voltage drop of spark switch when it turns on

$f_T$(Hz), working frequency of TENG

$V_{on}$, voltage of inductor when the spark switch is on and is also the input voltage of inductor

$V_{off}$, voltage of inductor when the spark switch is off and is also the output voltage of inductor.

$f_{sw}$(kHz), frequency of the spark switch

To successfully trigger the switch on, the voltage should satisfy the formula $V_B < V_{open}$.

In a working cycle, according to volt-second product law which refers to the product of the voltage of inductor when the switch is on and the corresponding switch on time equals the product of the voltage of inductor when the switch is off and the corresponding switch off time,

$$V_{on}T_{on} = V_{oFF}T_{oFF} \tag{1}$$

TENG can generate high voltage more than thousands of volts. The output voltage of inductor roughly equals the drive voltage of the external load which is mostly in the range between 1.5 V and 12 V. Therefore, there is a sharp decrease for the voltage on inductor after the switch off,

$$V_{oFF} \ll V_{on},\ T_{on} \ll T_{oFF} \tag{2}$$

We can further get,

$$\mathrm{D} = \frac{T_{on}}{T} = \frac{T_{on}}{T_{on}+T_{oFF}} \approx \frac{T_{on}}{T_{oFF}} = \frac{V_{oFF}}{V_{on}} \tag{3}$$

Therefore, D is far less than 1. Considering D is generally in the range from 0.2 to 0.5 for traditional EM, this EM based on inductor convertor for TENG is an extreme case.

**Note S2**

**Volume of magnetic core**

Here, to figure out a maximum output energy from EM unit as possible, we define a factor Z which is the ratio of core material permeability to effective permeability,

$$\mathrm{Z} = \frac{\mu_c}{\mu_e} \tag{4}$$

In which, $\mu_e$ is relative permeability of magnetic core when existing air gap and air gap can boost the stored energy in magnetic core generally; $\mu_c$ is the relative

permeability of the core without air gap.
The stored energy of inductor with a magnetic core gap $E_{gc}$ is

$$E_{gc} = \frac{B^2 \times V_e}{2\mu_c \mu_0} \times Z \quad (5)$$

Where B is magnetic induction intensity, $V_e$ is the volume of magnetic core, $\mu_0$ is vacuum permeability of magnetic core.
PC40 is a common material for magnetic core used in switch power supply and has a low cost. Here, the relative permeability $\mu_c$ for our used PC40 magnetic core is 2300. Generally, the actual magnetic core size is a little larger than the theoretical value to achieve a high output energy. In addition, there are saturation flux density $B_s$ and residual flux density $B_r$ existing for a core. The actual stored energy is

$$E_{gc} = \frac{(B_S^2 - B_r^2) \times V_e}{2\mu_c \mu_0} \times Z \quad (6)$$

To achieve a high energy conversion efficiency, the maximum energy that the inductor can accommodate should be no less than the energy $E_{in}$ from TENG,

$$E_{gc} \geq E_{in} \quad (7)$$

From Equations 6 and 7, we can get,

$$\frac{(B_S^2 - B_r^2) \times V_e}{2\mu_c \mu_0} \times Z \geq E_{in} \quad (8)$$

$$V_e \geq \frac{2E_{in} \cdot \mu_c \mu_0}{(B_S^2 - B_r^2) \cdot Z} \quad (9)$$

$B_r$ can be neglected due to the introduce of air gap in core. So, the effective volume of magnetic core satisfies the follow equation,

$$V_e \geq \frac{2E_{in}(J) \mu_c \cdot \mu_0}{B_S^2(T) \cdot Z} \times 10^9 \quad \text{mm}^3 \quad (10)$$

The vacuum permeability $\mu_0$ is $4\pi \times 10^{-7}\ \text{H} \cdot m^{-1}$. Saturation flux density $B_s$ is 0.51 T at room temperature and is 0.39 T at 100℃. We adopt value of 0.4 T for convenience in the next calculation.
In addition, the output energy $E_T$ of TENG through the spark switch is

$$E_{in} = \frac{1}{2}(V_B - V_{Dair}) \cdot Q_{on} \quad (11)$$

In this work, the turn on voltage for spark switch is 6, 000 V with a 500 V voltage drop. And the charge flows through the spark switch is 400 nC when the switch is on. We calculated the energy output from TENG to the inductor by integrating the voltage-charge plot (Figures 2D and 2E), and it is 1.08 mJ, which is consistent with equation 11. Combining Equation 10 and 11, we can get the minimum core volume for TENG is:

$$V_e \geq \frac{(V_B(V) - V_{Dair}(V)) \cdot Q_{on}(C) \cdot \mu_c \mu_0}{B_S^2(T) \cdot Z} \times 10^9 \quad \text{mm}^3 \quad (12)$$

For EM unit using inductor, the empirical value of Z is in the range between 10 and 40. The current ripple coefficient of TENG is quite large and sets a high requirement for the conductive wire. Besides, a large Z leads to a large coil number which could beyond the limit that the magnetic core can accommodate. Hence, we choose a medium Z as 25 in the calculation. From Equation 11, we can get the minimum magnetic core volume

is 1560 $mm^3$. Thus, EE22 with 1629 $mm^3$ volume can meet the requirement.

**Note S3**

**Cross sectional area of conductor and skin effect**

Here, we discussion total cross-sectional area of conductor $A_{Cu}$. From the formulas $A_{Cu} = \frac{\Delta I}{I_J}$ and $\Delta I = I_{pk} = 2I_L$, we can know $I_L$ is the key to get the $A_{Cu}$.

The goal for EM of TENG is to enhance the constant current to drive portable electronic devices continuously. Here, we define the drive current on devices at the optimum output condition,

$$I_{drive} = \frac{E_{in} \times \eta}{V_{drive}} \times f_T \tag{13}$$

$V_{drive}$ is the drive voltage for device, $\eta$ is the energy efficiency for TENG using EM.

On the other hand, the output charge from inductor equals to the consumed charge of the external load,

$$\frac{I_L}{f_{sw}} = \frac{I_{drive}}{f_T} \tag{14}$$

Combine Equations 13 and 14, we obtain.

$$I_L = \frac{f_{sw} \eta E_{in}}{V_{drive}} \tag{15}$$

So we can get the $A_{Cu}$ as:

$$A_{Cu} = \frac{2 f_{sw}(kHz) \times E_{in}(J)}{I_J(A/mm^2) \times V_{drive}(V)} \times 10^3 \ (\mathrm{mm}^2) \tag{16}$$

Where $I_J$ is current density; $I_{pk}$ is the peak value of current; $\Delta I$ is the difference between the peak value and the minimum vale of current; $I_L$ is median current; $V_{drive}$ is the drive voltage of device.

And the minimum conductor diameter when use a single strand wire is.

$$\mathrm{d} = 2\sqrt{(\frac{A_{Cu}}{\pi})} \ \mathrm{mm} \tag{17}$$

Considering the very low working frequency for TENG, the heating problem can be neglected. And larger current can flow through conductive wire. Here, we calculated the diameter of the wire at 10 A/$mm^2$ current density in the wire. Moreover, we found that the switch frequency from 2 to 15 kHz is suitable for the superhigh voltage electrostatic energy due to the very small duty ratio, and here we design the energy management unit at 5 kHz. From equation 12, the minimum size of the wire is calculated as 0.216$mm^2$, which is 0.5 mm diameter for a single strand wire. In addition, the conductor cross-sectional area for wire in 0.1×20 and 0.1×30 wires are 0.157 $mm^2$ and 0.236$mm^2$, respectively.

Skin effect is another impact factor in choosing the conductive wire, and is a common phenomenon in the conductive wire at high frequency. Under the action of electromagnetic induction, high-frequency current will produce eddy current in the conductor. With the increase of frequency, the central current density will decrease and the current density near the surface will increase, that is, the current is concentrated on the surface of the conductor, resulting in a sharp increase in the effective resistance of

the conductor.

Under the condition of meeting the cross-sectional area of conductor, usually, multi strand conductor is generally preferred rather than single strand conductor to effectively avoid the adverse effect of skin effect. In practical, the diameter d of single strand conductor shall be less than or equal to twice the skin depth Δ, i.e. $d \leq 2\ \Delta$; If not, the inductor shall be wound with a multi strand wire and for the diameter of each signal wire, it is less than twice the skin depth.

The skin depth for copper wire at 50℃ is

$$\Delta = \frac{70.1}{\sqrt{f_{sw}(Hz)}}\ (mm) \tag{18}$$

The skin depth calculated from the frequency of spark switch is 0.99 mm. So, in theory, the skin effect can be neglected.

However, from Figure 3A, it is a better output by using wire in multi strand wire, indicating that the high voltage electrostatic energy management is very different from the traditional power management in terms of AC impedance, which needs further exploration and correction.

**Note S4**

**A suitable magnetic core air gap**

In EM unit, inductor plays a key role in the energy conversion process. Inductor can store energy and enhancing the energy storage ability of inductor can further enhance the output energy from EM unit. Adding magnetic core gap is a general way to enhance the energy storage ability of inductor. By adding magnetic core gap, the reluctance increases while the effective magnetic permeability decreases, and in this way, the stored energy increases.

The relative permeability of magnetic core $\mu_e$ after adding magnetic core is

$$\mu_e = \frac{\mu_c}{1+\mu_c \times \frac{\delta}{l_e}} \approx \frac{l_e}{\delta} \tag{19}$$

In which, $\delta$ is air gap length; $l_e$ is the length of magnetic circuit of magnetic core.

To reduce magnetic flux leakage and enhance the energy storage ability of inductor, the air gap length $\delta$ should satisfy the formula

$$\delta \ll l_e \tag{20}$$

And from Equations 5 and 19, we obtain the air gap length is

$$\delta = \frac{Z l_e}{\mu_c} \tag{21}$$

For EE22, $L_e$ is 4.41 cm and Z is 25. Hence, we can get the air gap length $\delta$ for EE22 magnetic core is 0.48 mm. In addition, for EE16, EE28 and EE40, $\delta$ is 0.415 mm, 0.562 mm and 0.852 mm, respectively.

**Note S5**

**Minimum inductance and the coil number**

Generally, in the design process of the EM unit, the inductance is hard to be obtained directly, and it is usually calculated by some empirical parameters. Inductance L has some relationship with ripple coefficient r as follow,

$$L = \frac{V_{on} \times D}{r \times I_L \times f_{sw}} \tag{22}$$

In the EM process of TENG, the current on inductor firstly increases sharply when the spark switch is on and decreases to zero during the switch off time. This is a continuous conduction mode for inductor and the ripple coefficient r can be adopted as 2.
Thus, the minimum inductance is calculated as,

$$L = \frac{V_{on}(V) \times D \times V_{drive}(V)}{2\eta E_{in}(J) \times f_{sw}^2(KHz)} \times 10^{-3} \quad \text{(mH)} \tag{23}$$

From the inductance equation of inductor with air gap and Equation 4, we can get.

$$\mathrm{L} = \frac{\mu_e \mu_0 A_e}{l_e} N^2 = \frac{\mu_c \mu_0 A_e}{Z l_e} N^2 \tag{24}$$

Where $A_e$ is the total cross-section area of conductive wire.
And we can further get the coil number N

$$\mathrm{N} = \sqrt{\frac{Z l_e(mm)}{\mu_c \mu_0 A_e(mm^2)} L(mH)} \tag{25}$$

Due to the very small duty ratio in the energy management process for TENG, the transformation ratio is very large. Here, the frequency of spark switch is roughly at 5 kHz. Considering 5 V is a common standard output voltage for devices, we design this energy management with 5 V output voltage demand with a setting energy efficiency as 85%. At these conditions and from equation 23, the calculated inductance L is 0.589 mH. Hence, the corresponding coil number for EE22 is 78. And coil number for EE16 EE28 and EE40 are 102, 56 and 52.6 respectively.

From the detailed discussion above, due to the complexity of the whole system, it is noted that the design of energy management module not only needs the support of theory, but also the accumulation of experience. It is also indispensable to further explore the application of energy management for TENG.

## Reference


1.F. Xi, Y. Pang, W. Li, T. Jiang, L. Zhang, T. Guo, G. Liu, C. Zhang and Z. L. Wang, *Nano Energy*, 2017, **7**, 168-176.

2.H. Qin, G. Cheng, Y. Zi, G. Gu, B. Zhang, W. Shang, F. Yang, J. Yang, Z. Du and Z. L. Wang, *Advanced Functional Materials*, 2018, **28**.

3.X. Liang, T. Jiang, G. Liu, T. Xiao, L. Xu, W. Li, F. Xi, C. Zhang and Z. L. Wang, *Advanced Functional Materials*, 2019, **29**.

4.W. Harmon, D. Bamgboje, H. Guo, T. Hu and Z. L. Wang, *Nano Energy*, 2020, **71**.

5.X. Liang, T. Jiang, G. Liu, Y. Feng, C. Zhang and Z. L. Wang, *Energy & Environmental Science*, 2020, **13**, 277-285.

6.H. Zhang, F. Marty, X. Xia, Y. Zi, T. Bourouina, D. Galayko and P. Basset, *Nat Commun*, 2020, **11**, 3221.

7.W. Shang, G. Gu, W. Zhang, H. Luo, T. Wang, B. Zhang, J. Guo, P. Cui, F. Yang, G. Cheng and Z. Du, *Nano Energy*, 2021, **82**.

8.L. Long, W. Liu, Z. Wang, W. He, G. Li, Q. Tang, H. Guo, X. Pu, Y. Liu and C. Hu, *Nat Commun*, 2021, **12**, 4689.